Oxygen transport and dynamic surface tension of liquid metals

The Royal Society

Phil. Trans. R. Soc. Lond. A 1998 **356**, 857-870
doi: 10.1098/rsta.1998.0192

Oxygen transport and dynamic surface tension of liquid metals

By Enrica Ricci[1], Lorenzo Nanni[2] and Alberto Passerone[1]
[1]*Istituto di Chimica Fisica Applicata dei Materiali, MITER-CNR, Via De Marini 6, 16149 Genova, Italy*
[2]*ISTIC, University of Genova, Via all'Opera Pia 15, 16145 Genova, Italy*

Theoretical models have been developed to study the behaviour of liquid metal surfaces in the presence of gaseous surface active elements, relating the mass exchange between the liquid metal and the surrounding atmosphere under the Knudsen regime. Steady-state conditions can be defined for which an 'effective oxidation pressure' is formulated, providing a useful means for a sound choice of the most convenient conditions for oxygen-free high-temperature surface tension measurements. The experimental results presented here concern dynamic surface tension measurements in a time window ranging from half a second to hours. They confirm the theoretical predictions of the model and reveal unexpected behaviours of the liquid surface when subjected to different temperature profiles.

Keywords: surface tension; liquid tin; liquid metals; oxygen adsorption

1. Introduction

When an interface between two immiscible fluids is subjected to a temperature (or concentration) gradient, its interfacial tension varies from point to point: these gradients along the surface induce shear stresses that result in fluid motion. For a pure liquid in a temperature field parallel to the surface, there is a flow from the hot end towards the cold end. Since bulk fluids are viscous, they are dragged along: thus, bulk fluid motion results from interfacial temperature or concentration gradients (thermocapillary or solutocapillary effects). The velocity profile, which is a function of the vertical distance of the free surface (or the interface) from the base plane can attain a maximum velocity ranging from some mm s^{-1} to several cm s^{-1}, depending on the surface tension temperature coefficient and on the liquid viscosity.

The phenomena arising from interfacial tension gradients are collectively termed 'Marangoni effects', after the Italian physicist Carlo Marangoni (1840–1925) who published a series of papers on this subject between 1871 and 1878 (Marangoni 1871, 1872, 1878).

These phenomena can be found in the presence of mass transfer and affect liquid–liquid extraction, bubbles, drop migration and the spreading of lubricants. Marangoni motion is also responsible for wall erosion in glass-melting furnaces, and influences crystal growth processes, foam stability, and the stability of liquid layers.

In the particular field of metallurgy, welding procedures are highly affected by surface tension driven motions: the penetration of the liquid phase depends to a great extent on the surface and bulk movements of the liquid pool. The presence of surface active elements, like oxygen and sulphur in liquid iron, changes in a dramatic way the liquid surface tension and its temperature dependence (see Keene 1988), so that the liquid can flow not only with very different velocities but also the direction of flow can be reversed, due to changes in the surface tension coefficient from negative to positive (Desré & Joud 1981).

Thus, considering the importance of surface tension variation as a function of temperature and composition, the high surface activity of oxygen and the scarcity of experimental data on liquid metal systems, we focused our attention on the thermodynamic and kinetic aspects of the oxygen mass transfer at the liquid–vapour interface, relating predictive theoretical models to the experimental results arising from dynamic surface tension measurements of liquid metals by the sessile drop technique.

2. Theoretical approach

Fluid-dynamic models of oxygen mass exchange under very low total pressures have already been developed (Castello *et al.* 1994; Laurant *et al.* 1988) taking into account that, in the Hertz–Knudsen diffusion regime, the mean free path of the molecules in the gas phase is large with respect to the dimensions of the reactor. As a consequence, when metals able to form volatile oxides are considered (see Kellogg 1966), condensation of the oxide vapours on the reactor walls can rapidly occur. In general, any kind of removal of oxide vapours from above the metal surface (pumping, condensation on cold surfaces) can cause significant displacements of the oxidation equilibrium at the gas–liquid interface, by enhancing the rate of the vaporization of the condensed oxide (Brewer & Rosemblatt 1962).

Let us consider a typical experiment of surface tension measurement under a vacuum: the liquid metal sample is placed in a closed chamber at a temperature T, under a total pressure P_{tot} lower than 1 Pa; the oxygen residual pressure $P_{\mathrm{O_2,g}}$ is considered constant. Above the oxygen solubility limit in the liquid metal, $x_{\mathrm{O,s}}$, the formation of the first stable oxide in the condensed phase is favoured thermodynamically. When the metal and the oxide coexist in the condensed phase, the atmospheric composition is fixed at constant T for the system at equilibrium and it can be calculated from thermochemical data. Moreover, the vapour pressures $P_{j,s}$ of the species containing oxygen resulting from thermal decomposition of the oxide depend exclusively on T. Under these conditions, the oxygen mass transfer between the gas and the condensed phase can be formalized through the evaluation of the global flux to and from the surface. There are two contributions to the oxygen total flux: one given by 'free' molecular oxygen and the other one due to the j species, where oxygen is 'linked' as a chemical compound.

It can be demonstrated (Castello *et al.* 1994) that a steady-state condition with respect to the oxygen exchange is reached when the oxygen residual pressure is equal to the quantity

$$P^{\mathrm{E}}_{\mathrm{O_2,s}} = P_{\mathrm{O_2,s}} + \sum_j v_j \frac{\alpha_j}{\alpha_{\mathrm{O_2}}} (m + v_j)^{-1/2} P_{j,s} \tag{2.1}$$

where v_j is the stoichiometry coefficient of the jth oxide formation reaction, $P_{\mathrm{O_2,s}}$ is the oxygen equilibrium pressure, $P_{j,s}$ is the vapour pressure of the species containing oxygen, α_i is the sticking coefficient of the species i and m is the ratio of the molecular weights.

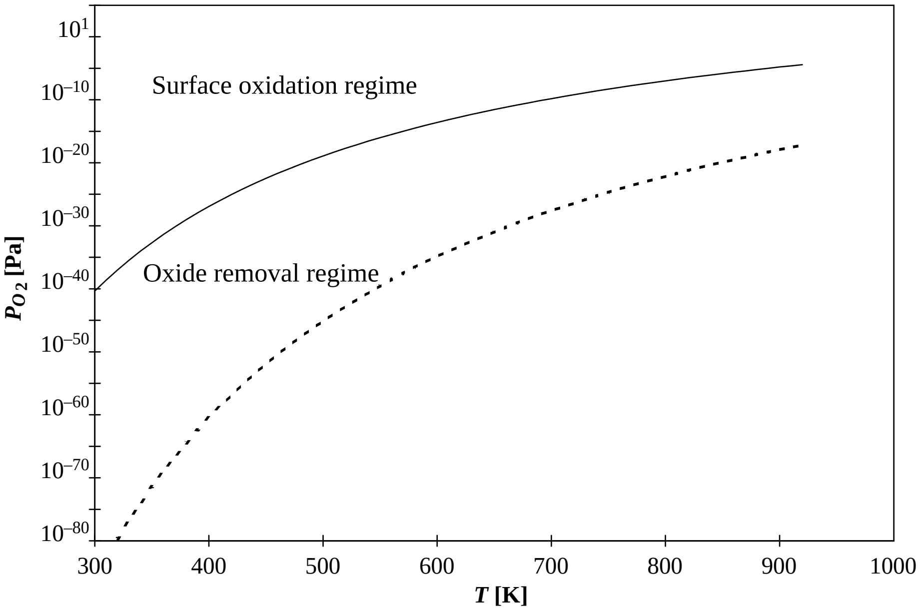

Figure 1. Effective oxidation pressure $P^{\mathrm{E}}_{\mathrm{O_2,s}}$ (bold line) and equilibrium oxygen pressure $P_{\mathrm{O_2,s}}$ (dotted line) versus T curves for the tin–oxygen system calculated at saturation.

This equation defines the 'effective oxidation pressure' at saturation ($P^{\mathrm{E}}_{\mathrm{O_2,s}}$): it is the oxygen pressure that has to be imposed in order to maintain in a steady state a metal sample completely saturated with oxygen and it applies for the oxidation of liquid and solid metals under vacuum conditions. Owing to the contribution of the volatile oxides to the total oxygen loss, the effective saturation pressure $P^{\mathrm{E}}_{\mathrm{O_2,s}}$, can be several orders of magnitude larger than the corresponding saturation value under conditions of thermodynamic equilibrium between the gas and the condensed phase, as shown in figure 1 for the tin–oxygen system.

The $P^{\mathrm{E}}_{\mathrm{O_2,s}}$ versus T curve can be regarded as a 'transition curve' between the two regimes: an 'oxygen removal regime' where the metal surface loses oxygen, through the formation of compounds that evaporate rapidly; and, on the other side, a 'surface oxidation regime' where a thermodynamically stable oxide layer is expected to appear on the surface.

An extension of the model briefly described above, allows the interfacial characteristic times (for diffusion, and to reach stationary conditions) and the trend of the interfacial composition versus time to be evaluated. To this end, the theory (Ricci *et al.* 1998) takes into account both the local oxygen mass balance in a liquid metal drop assumed as a rigid sphere under Knudsen conditions, and the total mass balance.

The diffusion time within the drop is

$$t_{\mathrm{D}} = \frac{R^2}{9D_{\mathrm{O}}} \tag{2.2}$$

and the characteristic time at steady-state conditions is

$$t_{\mathrm{st}} = \frac{1}{3}\frac{Rc_{\mathrm{l}}}{N^{0}_{\mathrm{O_2,I}}}(x^{0}_{\mathrm{O}} - x^{\mathrm{st}}_{\mathrm{O}}), \tag{2.3}$$

where t_{st} is the time necessary for a homogeneous drop to reach the steady-state

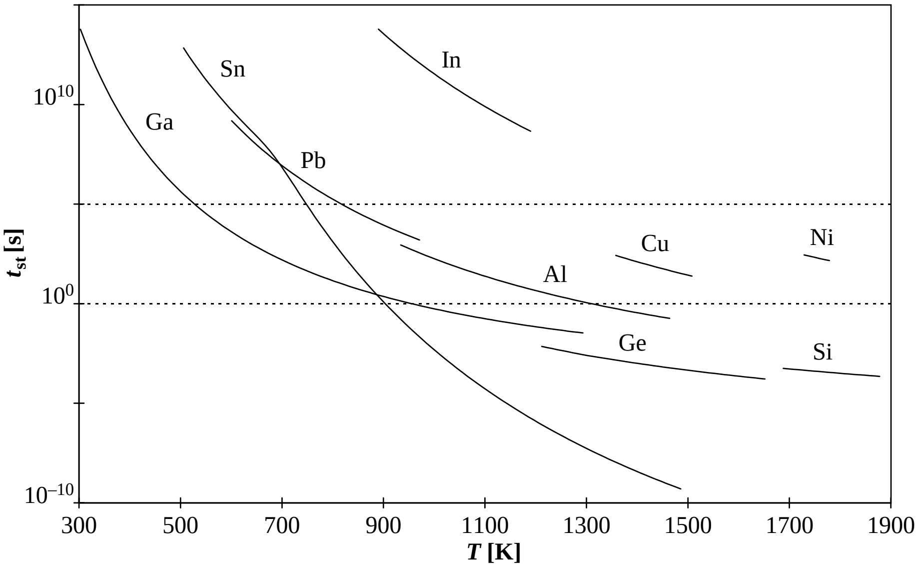

Figure 2. Characteristic times versus temperature for different liquid metal systems between melting and boiling points at a total pressure $P_{\text{tot}} = 1$ Pa. The observable times lie between the two dotted lines.

composition x_{O}^{st}; R is the drop radius, c_{l} is the liquid bulk concentration and $N^{0}_{\text{O}_2,\text{I}}$ is the initial oxygen flux at the interface.

When the case of nonlinear flux is considered, as in the conditions of the Knudsen regime, and when the saturation values of oxygen pressure and the vapour pressure of species containing oxygen are imposed (oxygen saturation, with the system in monovariant equilibrium, equation (2.1)), the characteristic time can be calculated by the relationship

$$t_{\text{st}} = \frac{Rc_{\text{l}}x_{\text{O,s}}}{3k_{\text{O}_2}P_{\text{O}_2,\text{s}}}\left(1+\sum_{j} v_j \frac{\alpha_j}{\alpha_{\text{O}_2}}\frac{1}{\sqrt{m+v_j}}\frac{P_{j,s}}{P_{\text{O}_2,\text{s}}}\right)^{-1}, \tag{2.4}$$

where k_{O_2} is the oxygen partial transport coefficient.

The calculated values of the characteristic times as a function of temperature between melting and boiling points for a set of selected metals, considering a metal drop sample of radius $R = 0.5$ cm under a total pressure of 1 Pa, are reported in figure 2. The two dotted lines delimit the time range observable within our experimental set-up (from 1 s to several hours). Among the metals whose curves lie in this range, Sn, Ga and Al seem to be the most convenient to be used as 'test systems'. In the following, the experimental results on liquid tin are presented. Tin has been chosen due to its low melting point and its low vapour pressure, which offers the opportunity to work over a wide temperature range.

3. Experiment

A fast automatic procedure, Automatic Surface-Tension Real-time Acquisition (ASTRA), has been recently designed and setup in our laboratory (Liggieri & Passerone 1989; Ravera *et al.* 1997) allowing the surface tension of liquid metals and alloys to be measured, in a time frame ranging from half a second to hours. In this way, the variation of surface tension with time can be recorded, giving access to the experimental study of dynamic phenomena at liquid surfaces, in particular of adsorption, both from the liquid and the gaseous side.

The experimental setup consists of a vacuum chamber, working both at 10^{-5} Pa and under controlled atmosphere, in which the metallic specimen is introduced by means of a magnetic device; a high quality optical line with a CCD camera; an ion-gun to clean the specimen surface also in the liquid state. The oxygen partial pressure is monitored by means of a solid state oxygen gauge. The metallic specimen is supported on a sapphire cup, especially designed to help maintain the axial symmetry of the sessile drop and to avoid any chemical contamination of the liquid phase.

The experimental reproducibility in measurements of surface tension was found to be ±0.1%, making this the most precise technique for measuring liquid state surface tensions.

Basically, three kinds of experiments have been made, giving access to the dynamic conditions of the liquid tin surface:

(A) at constant temperature, under different oxygen partial pressures, in order to check the calculated value of the effective oxidation pressure $P^{\mathrm{E}}_{\mathrm{O_2,s}}$;

(B) on 'oxidized' samples, in order to check the effectiveness of the ion-etching procedure to clean the liquid tin surface;

(C) at constant oxygen pressure, but with temperature varying with different gradients, in order to check the response of the surface (through surface tension variations) to the environmental dynamics.

4. Results and discussion

(*a*) *Experiments at constant temperature*

The results of two significant experiments, made under essentially the same conditions, i.e. $T = 818$ K and $P_{\mathrm{O_2}}$ varying between 10^{-7} and 10^{-1} Pa, are reported here.

Figure 3 shows the results of the variation of the surface tension with time for a liquid tin drop, previously ion-etched ($E = 5$ KeV; $I = 25$ μA) in the liquid state for about 20 min. Figure 4 shows the conditions of oxygen partial pressure and temperature during the experiment.

From the moment of melting, the liquid metal drop under an oxygen partial pressure of 10^{-7} Pa (point 1 in figures 3 and 4) has a surface tension $\gamma = 533\ \mathrm{mN\ m^{-1}}$, which remains constant until the imposed oxygen pressure increases to 10^{-1} Pa (point 2 in figures 3 and 4). As shown in figure 4, this variation crosses the $P^{\mathrm{E}}_{\mathrm{O_2,s}}$ curve, showing that the system goes from the 'oxygen removal' regime to the 'surface oxidation' regime. The surface tension value starts decreasing at the same time, reaching the value $\gamma = 498\ \mathrm{mN\ m^{-1}}$. However, when the oxygen pressure is lowered down to 10^{-5} Pa (point 3 in figures 3 and 4), the surface tension no longer varies, even if the representative point lies just under the curve, i.e. in the 'oxide removal' region. Such a behaviour, found also in other experiments, is due to the intrinsic stability of the 'oxide layer' coating the liquid metal surface.

Indeed, if the surface is ion-etched under the same low oxygen pressure, the surface tension immediately increases eventually reaching a value close to the initial one. The results of such a behaviour are reported in figure 5; in figure 6 the corresponding oxygen partial pressure conditions during the experiment are shown. Also in this case, starting from an imposed oxygen partial pressure of 10^{-7} Pa, i.e. the 'oxide

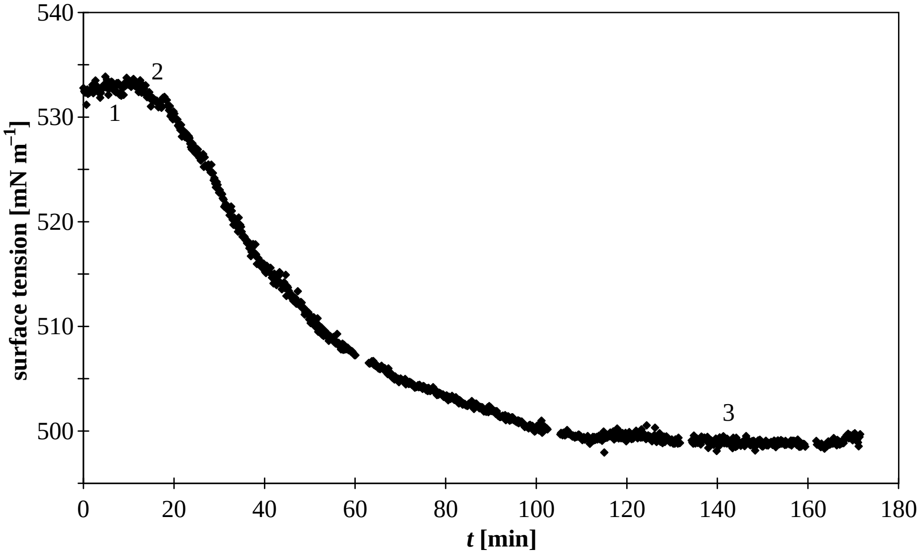

Figure 3. Surface tension versus time plot for liquid tin at $T = 818$ K and varying oxygen partial pressure: 1, $P_{O_2} = 10^{-7}$ Pa; 2, $P_{O_2} = 10^{-1}$ Pa; 3, $P_{O_2} = 10^{-5}$ Pa.

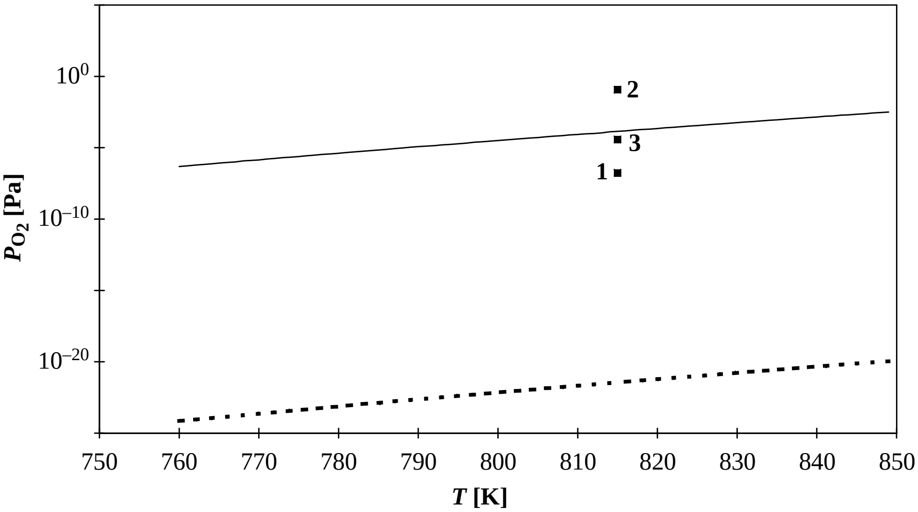

Figure 4. Temperature and oxygen partial pressure conditions of the experiment reported in figure 3: bold line, effective oxidation pressure; dotted line, equilibrium oxygen pressure.

removal' regime (point 1 in figures 5 and 6), the value of the surface tension is $\gamma = 533\,\mathrm{mN\,m^{-1}}$, which indicates a 'clean' system.

When the imposed oxygen pressure increases to 10^{-1} Pa (point 2 in figures 5 and 6), this variation crosses the curve, showing that the system goes from the 'oxygen removal' regime to the 'surface oxidation' regime and the surface tension value starts decreasing at the same time. Then, when the oxygen partial pressure is lowered down to 10^{-2} Pa (point 3 in figures 5 and 6), the surface tension continues to decrease but less rapidly than in the previous experiment. However, also in this case, when the oxygen pressure is lowered down to 10^{-5} Pa (point 4 in figures 5 and 6), the surface tension no longer varies, due to the stability of the surface coating

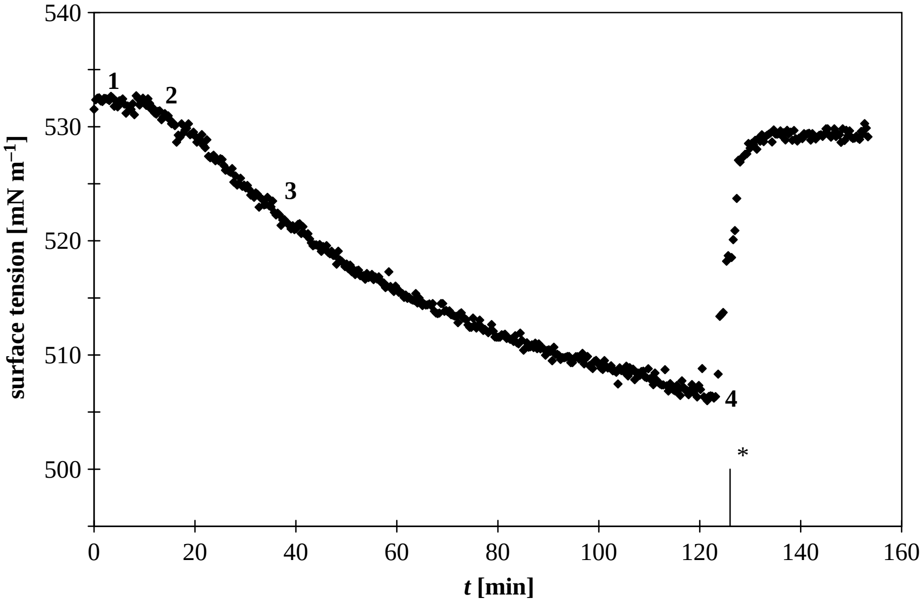

Figure 5. Surface tension versus time plot for liquid tin at $T = 818$ K and varying oxygen partial pressure: 1, $P_{O_2} = 10^{-7}$ Pa; 2, $P_{O_2} = 10^{-1}$ Pa; 3, $P_{O_2} = 10^{-2}$ Pa; 4, $P_{O_2} = 10^{-5}$ Pa; $*$, start of surface sputtering.

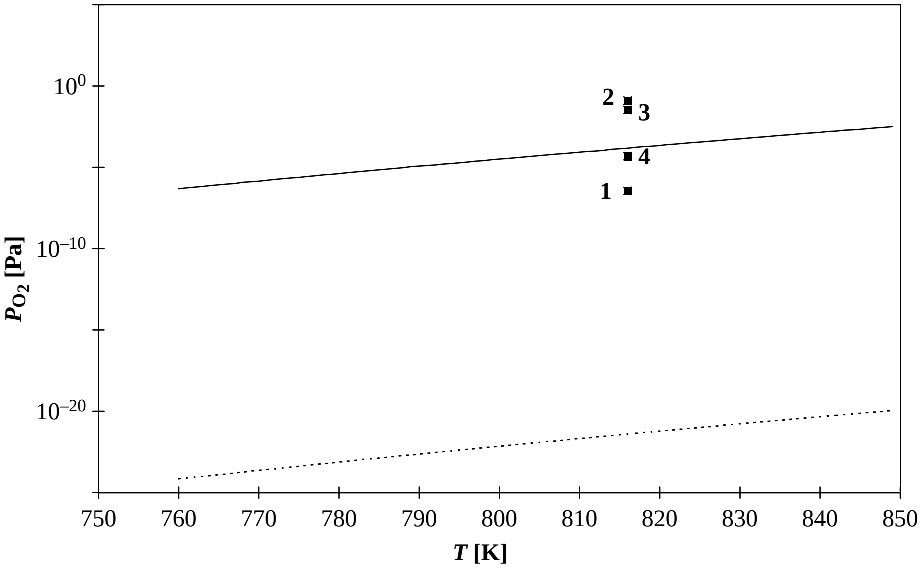

Figure 6. Temperature and oxygen partial pressure conditions of the experiment reported in figure 5: bold line, effective oxidation pressure; dotted line, equilibrium oxygen pressure.

oxide layer. However, an ion-etching of the liquid metal coated surface for about 10 min ($E = 5$ KeV; $I = 25$ μA) is sufficient to increase the surface tension up to a value very close to the initial one. These results confirm the theoretical prediction of an 'effective saturation pressure' well above the thermodynamic one. The calculated oxygen partial pressure values defining the transition between 'oxidized' and 'cleaner' surfaces are in very good agreement with the measured values.

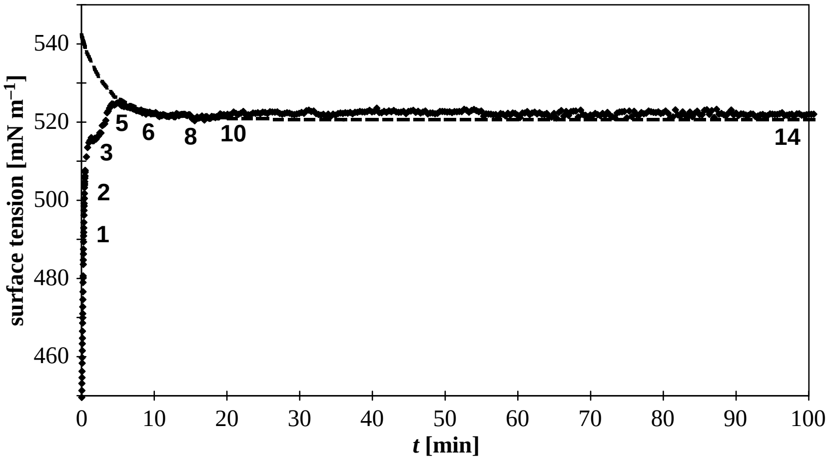

Figure 7. Surface tension versus time plot for liquid tin at $P_{O_2} = 10^{-7}$ Pa and varying temperature; the segment between 10 and 14 is nearly isothermal ($T = 818 \pm 3$ K). Dashed line, reference surface tension values ($\gamma = 560 - 0.125(T - T_m)$).

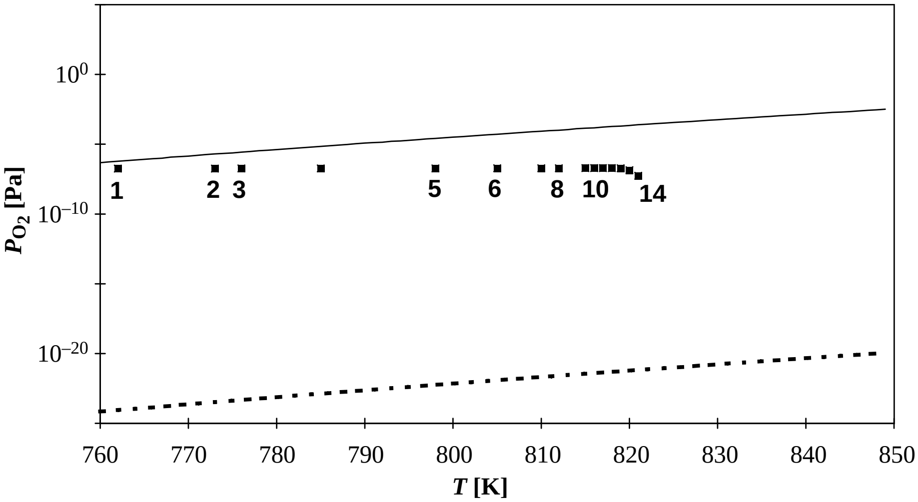

Figure 8. Temperature variation conditions at constant oxygen partial pressure ($P_{O_2} = 10^{-7}$ Pa) of the experiment reported in figure 7: bold line, effective oxidation pressure; dotted line, equilibrium oxygen pressure.

(*b*) *Experiments on 'oxidized' samples*

Some measurements have also been made on 'oxidized' samples, to follow the cleaning up of the liquid surface. A typical test is reported in figure 7. Figure 8 shows the corresponding oxygen pressure conditions. The tin sample was pretreated at $T = 823$ K and $P_{O_2} = 90$ Pa for 10 min in order to increase its bulk oxygen content; after quenching, the surface of the sample was cleaned both mechanically and chemically. This sample was then brought under a constant oxygen partial pressure of about 10^{-7} Pa ('oxide removal' regime). It should be noted that the temperature reaches a constant value of 820 K after about 15 min (point 10 in figures 7 and 8). During the first 5 min (from points 1–5 in figures 7 and 8) the value of surface tension rapidly increases corresponding to a decrease of the oxygen content inside the drop.

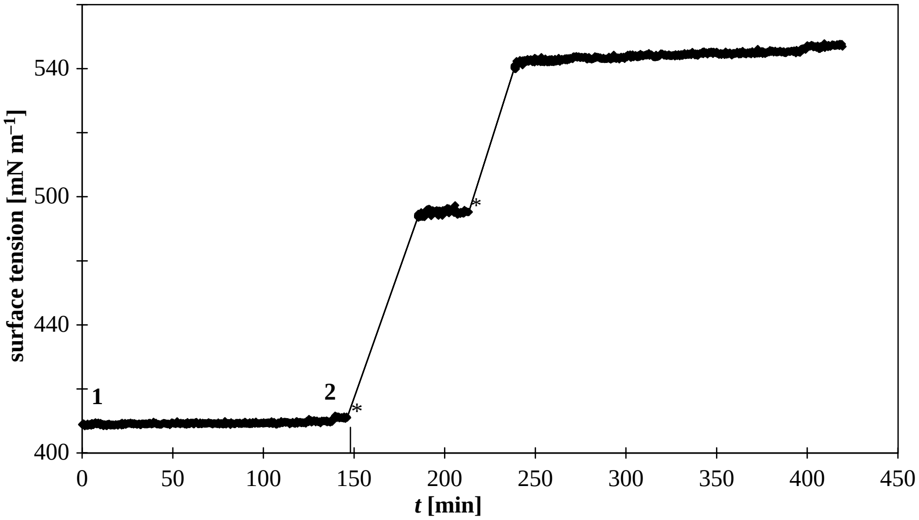

Figure 9. Surface tension versus time plot for liquid tin at $T = 821$ K and varying oxygen partial pressure: 1, $P_{O_2} = 10^{-7}$ Pa; 2, $P_{O_2} = 10^{-1}$ Pa; $*$, start of surface sputtering.

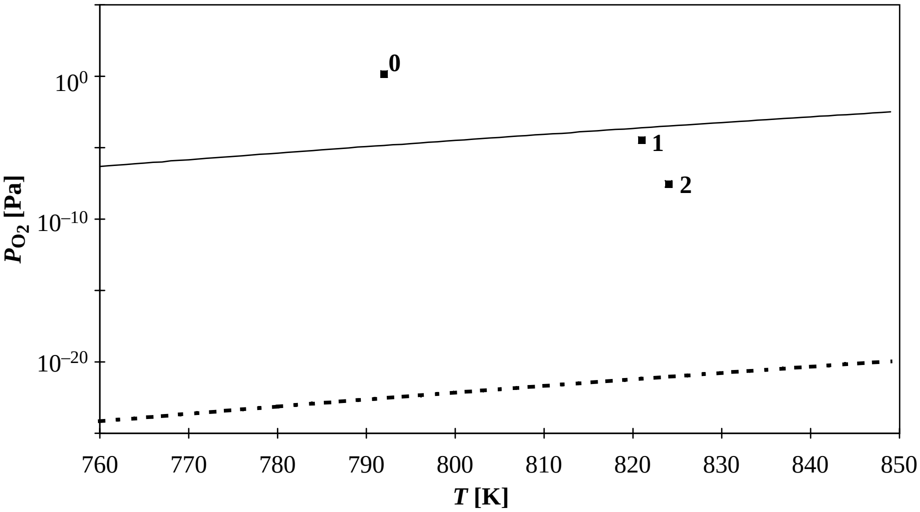

Figure 10. Temperature and oxygen partial pressure conditions of the experiment reported in figure 9. (0 = initial 'oxidized' condition): bold line, effective oxidation pressure; dotted line, equilibrium oxygen pressure.

After this time the experimental data agree very well with the literature (dotted line); the surface tension value remains constant for several hours showing that the clean liquid surface is thermodynamically stable under these conditions.

A further confirmation of the effectiveness of the ion-etching procedure in cleaning the liquid tin surface is shown in figures 9 and 10. Also in this case the sample was put initially under oxidizing conditions starting at $T \approx 790$ K and $P_{O_2} = 1$ Pa for 30 min (point 0 in figure 10) and then brought directly into the 'oxide removal' regime by slightly increasing the temperature (up to $T = 821$ K and $P_{O_2} = 10^{-5}$ Pa: point 1 in figures 9 and 10). When the system enters this region the liquid surface does not react at all: the surface tension remaining constant for nearly 2.5 h. But, as soon

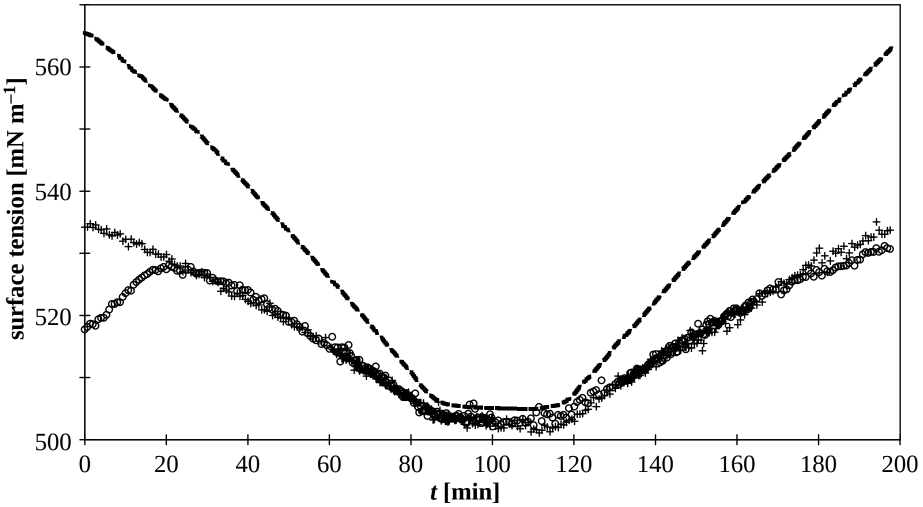

Figure 11. Surface tension versus time variation at 5 K min^{-1} between 625 and 1100 K at different oxygen partial pressures: run 12 (○), $P_{O_2} = 10^{-3}$ Pa; run 14 (+), $P_{O_2} = 10^{-15}$ Pa; dashed line, surface tension values ($\gamma = 581 - 0.13(T - T_m)$) from Passerone *et al.* (1990).

as the ion-etching process is started, the surface tension increases very quickly, as clearly shown in figure 9, and the pressure value decreases spontaneously by three orders of magnitude (point 2 in figures 9 and 10). The increase in surface tension seems to be linearly related to the sputtering time.

If the system is left free to evolve after the etching procedure, the surface tension keeps increasing towards the before mentioned literature value, as expected in the 'oxide removal' regime.

(*c*) *Experiments at constant oxygen partial pressure*

The temporal evolution of surface tension of liquid tin as a function of temperature in the range between 625–1100 K under an imposed constant oxygen partial pressure has been also investigated. In figure 11, the results of two runs, carried out under these conditions and at the same temperature variation rate ($\nabla T = 5$ K min^{-1}) are reported, while the corresponding oxygen partial pressure conditions are reported in figure 12. The initial conditions of run 12 fall in the 'surface oxidation' regime below 820 K, while run 14 was carried out in the 'oxide removal' region in the whole temperature range.

The surface tension results, recorded both during the heating up and the cooling down periods, show a strikingly linear behaviour as a function of temperature, without any hysteresis effect: the surface tension temperature coefficients coincide, in the same experiment, during heating and cooling. The different behaviour during the first 20 min of the two runs depends on the different initial oxygen partial pressure conditions imposed. From this time on, even if made in the 'surface oxidation' regime below $T = 820$ K, run 12 has shown surface tension variations which replicate exactly those found in run 14, which instead pertains completely to the 'oxide removal' regime.

Indeed, under dynamic conditions (very low total pressure, gas flow at low oxygen partial pressure), the oxygen exchange between the liquid surface and the environment is highly dependent on the rate of temperature variations to which the liquid surface is subjected. This appears clearly in figure 13 in which the results of run

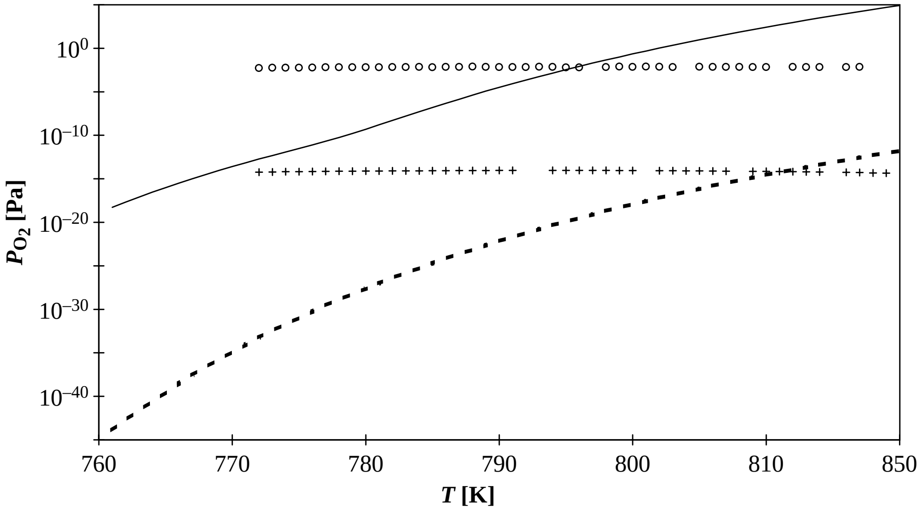

Figure 12. Temperature and oxygen partial pressure conditions of the experiment reported in figure 11: run 12, (○); run 14, (+); bold line, effective oxidation pressure; dotted line, equilibrium oxygen pressure.

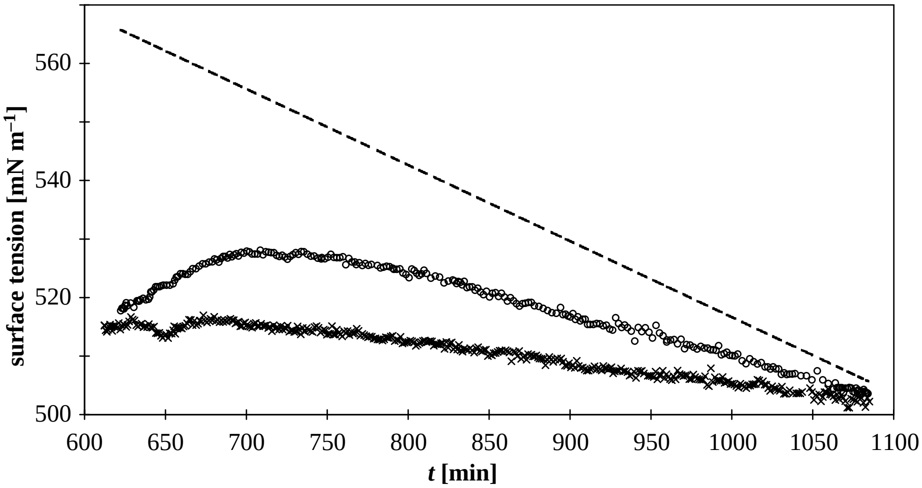

Figure 13. Surface tension versus temperature between 625 and 1100 K at the same oxygen partial pressure, $P_{O_2} = 10^{-1}$ Pa, but different temperature variation rates: run 12 (○), 5 K min^{-1}; run 16 (×), 1 K min^{-1}; dashed line, surface tension values ($\gamma = 581 - 0.13(T - T_m)$) from Passerone *et al.* (1990).

12 and run 16 are compared. They were carried out at the same oxygen partial pressure conditions but at different temperature variation rates, 5 and 1 K min^{-1}, respectively.

It should also be noted that all runs (12, 14 and 16) reach, in the high-temperature limit ($T = 1088$ K), the same high surface tension value ($\gamma = 503$ mN m^{-1}) which is very close to the mean of the reported literature values (Passerone *et al.* 1990). This means that, at high temperature, the liquid surface attains the conditions foreseen by the theoretical model, irrespective of the heating rate; the effect of the temperature gradient becoming relevant at lower temperatures. This behaviour is further

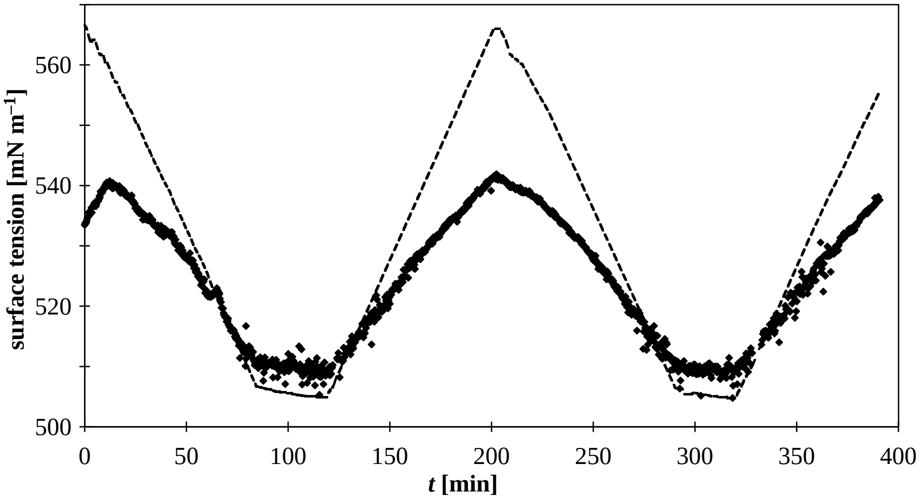

Figure 14. Surface tension versus time variation at 5 K min^{-1} in a double cycle between 625 and 1100 K at constant oxygen partial pressure, $P_{O_2} = 10^{-3}$ Pa: dashed line: surface tension values ($\gamma = 581 - 0.13(T - T_m)$) from Passerone *et al.* (1990).

Table 1. *Surface tension values of tin at melting temperature as a function of imposed oxygen partial pressures and different temperature variation rates*

(In the last column, $T\uparrow$ and $T\downarrow$ denote temperature increasing and temperature decreasing, respectively.)

P_{O_2} (Pa)	∇T (K min^{-1})	γ_0 (mN m^{-1})	γ' (mN m^{-1})	stand. dev. on γ'	remarks	
10^{-3}	5	545.9	−0.073	7.1×10^{-4}	s.ox. → ox.rem.	$T\uparrow$
10^{-3}	5	545.6	−0.072	7.8×10^{-4}	ox.rem. → s.ox.	$T\downarrow$
10^{-3}	5	554.9	−0.076	5.8×10^{-4}	s.ox. → ox.rem.	$T\uparrow$
10^{-3}	5	552.6	−0.073	4.6×10^{-4}	s.ox. → ox.rem.	$T\uparrow$
10^{-3}	5	550.6	−0.071	4.7×10^{-4}	ox.rem. → s.ox.	$T\downarrow$
10^{-3}	5	552.1	−0.073	5.8×10^{-4}	ox. rem. → s.ox.	$T\downarrow$
10^{-3}	1	519.9	−0.037	4.3×10^{-4}	s.ox. → ox.rem.	$T\uparrow$
10^{-3}	1	522.6	−0.035	2.5×10^{-4}	s.ox. → ox.rem.	$T\uparrow$
10^{-3}	1	527.2	−0.044	5.9×10^{-3}	ox.rem. → s.ox.	$T\downarrow$
10^{-15}	5	543.2	−0.067	3.9×10^{-4}	oxide removal	$T\uparrow$
10^{-15}	5	545.5	−0.073	5.8×10^{-4}	oxide removal	$T\downarrow$

confirmed by the experiment shown in figure 14 aimed at confirming the complete reproducibility and reversibility of the surface conditions.

The operating conditions and the results of surface tension measurements of several experiments are collected in table 1. All of them have been made at constant oxygen partial pressure (P_{O_2}) in a temperature range between 625 and 1100 K, and at different temperature variation rates ($\nabla T = 1$ and 5 K min^{-1}).

The remarkable reproducibility of the γ versus $T\uparrow$ and $T\downarrow$ curves within the same class of experiment (1 and 5 K min^{-1}) clearly indicates that the fluid-dynamic characteristics of the oxygen exchange are the key factor in determining the surface tension variations.

5. Conclusions

On the basis of the results presented here the following conclusions can be drawn.

(1) The experimental technique (ASTRA) allows real-time surface tension data of liquid metal systems to be measured in a time-scale from 0.5 s to hours, with a precision of 0.1%. Thus, the dynamic behaviour of the liquid surface in various environments can be easily followed, and possible 'second-order' effects on surface tension can be detected.

(2) The theoretical prediction of an 'effective saturation pressure', usually many orders of magnitude higher than the thermodynamic prediction, is fully confirmed: this new limit can help explain the oxidation behaviour of liquid metals under a vacuum. Moreover, a precise definition of the operating conditions to achieve a clean surface can be given.

(3) The behaviour of liquid tin (and possibly of other liquid metals) with respect to surface oxidation depends, at constant temperature, on the fluid-dynamic regimes of metal and oxide vapours exchange (as monitored by the $P^{\mathrm{E}}_{\mathrm{O_2,s}}$ critical curve) and, at varying temperature, on its gradient with time.

(4) As Marangoni effects are driven by the surface tension variations with temperature and/or composition, special care has to be taken when using literature values. Indeed, the present study clearly shows that even if 'equilibrium' positive values are expected for γ' it may happen that, under dynamic conditions, these values change, not only in magnitude, but also in sign. From a technological viewpoint, the findings reported here imply that Marangoni motions are affected not only by temperature gradients but also, and to a large extent, by the rate imposed to temperature variations.

The contribution to the theoretical development of this work by Professor P. Costa and Professor E. Arato (ISTIC, University of Genova) is gratefully acknowledged.

References

Brewer, L. & Rosemblatt, G. M. 1962 *Trans. Met. Soc. AIME* **224**, 1268.

Castello, P., Ricci, E., Passerone, A. & Costa, P. 1994 *J. Mater. Sci.* **29**, 6104.

Desré, P. J. & Joud, J. C. 1981 *Acta Astronaut.* **8**, 407.

Keene, B. J. 1988 *Int. Mater. Rev.* **33**, 1.

Kellogg, H. H. 1966 *Trans. Met. Soc. AIME* **263**, 602.

Laurant, V., Chatain, D., Chatillion, C. & Eustathopoulos, N. 1988 *Acta Metall.* **36**, 1797.

Liggieri, L. & Passerone, A. 1989 *High Temp. Tech.* **7**, 80.

Marangoni, C. 1871 *A. Phys. Chem., Poggendorff* **143**, 337.

Marangoni, C. 1872 *Nuovo Cim.* ser. 2, **5/6**, 239.

Marangoni, C. 1878 *Nuovo Cim.* ser. 3, **3**, 50, 97, and 193.

Passerone, A., Ricci, E. & Sangiorgi, R. 1990 *J. Mater. Sci.* **25**, 4266.

Ravera, F., Liggieri, L., Ferrari, M. & Passerone, A. 1997 *IXth Int. Conf. on Surface and Colloids Sci. (IACIS), Sophia.*

Ricci, E., Nanni, L., Arato, E. & Costa, P. 1998 *J. Mater. Sci.* **33**, 305.

Discussion

J. Jeffes (*Imperial College, London, UK*). D. Richardson found the rate of oxygen transfer from gas to a levitated copper drop was very sensitive to surface contamination. Very small amounts of silicon formed a permanent layer of silica. This was overcome by solidifying the droplet while levitated, treating it with hydrofluoric acid and relevitated when the oxygen mass transfer was found to be ten times greater.

In the present experiments was it really proved that the tin surface was really clean? Was oxygen content of the surface determined?

E. Ricci. No surface analysis was performed on the molten tin drops.

However, experiments have been made where the liquid surface was ion-etched until the surface tension value reached the high value expected for ‘pure’ tin. The reproducibility and the reversibility of the results obtained in that way represents an indirect confirmation that the liquid surface was reasonably clean when its surface tension attained the highest values.